ELSEVIER

Applied Catalysis A: General 167 (1998) 11–22

APPLIED CATALYSIS A: GENERAL

Ammoxidation of 3-picoline over V_2O_5/TiO_2 (anatase) system. II. Characterisation of the catalysts by DTA, SEM, FTIR, ESR and oxygen and ammonia chemisorption

K.V. Narayana, A. Venugopal, K.S. Rama Rao, S. Khaja Masthan,
V. Venkat Rao, P. Kanta Rao*

Catalysis and Physical Chemistry Division, Indian Institute of Chemical Technology, Hyderabad 500 007, India

Received 8 January 1997; received in revised form 22 August 1997; accepted 22 August 1997

Abstract

In an earlier communication the ammoxidation activity of V_2O_5/TiO_2 catalysts with V_2O_5 loadings in the range 0.4–9.9 mol% was correlated to the average oxidation number of vanadium in the catalysts. In the present work, these catalysts were characterised by SEM, FTIR, ESR, DTA techniques and chemisorption of NH_3 and O_2. The scanning electron micrographs of the catalysts indicate that deposition of vanadium is taking place inside the mesopores of titania (anatase) up to 3.4 mol% V_2O_5 corresponding to a monolayer coverage. Beyond this loading neddle-like and bulk structures of vanadia appear probably on the external surface of the catalysts. The bands at 1010–1020 cm^{-1} appearing in the FTIR spectra of fresh catalysts are characteristic of highly dispersed monomeric VO_x units and two-dimensional structures. The FTIR spectra of the used catalysts are altogether different from those of the fresh catalysts suggesting that the active phase has been drastically modified during the course of the reaction. The ESR spectrum of 0.4 mol% V_2O_5 shows an eightfold well resolved hyperfine structure indicating that V^{4+} is in diluted conditions on anatase surface. As V_2O_5 content increases the hyperfine structure of ESR spectrum gets progressively smeared out due to strong coupling between V^{4+} dipoles. The results indicate that vanadium is in a highly dispersed distorted octahedral or square pyramidal geometry at 3.4 mol% corresponding to a monolayer coverage. The DTA curves contain endothermic peaks at 100–150°C and 630–675°C corresponding to desorption of adsorbed water and melting of vanadia particles and loss of oxygen from vanadia. Chemisorption of NH_3 and O_2 is observed to exhibit maximum at the monolayer V_2O_5 loading just as the ammoxidation activity of the catalysts. © 1998 Elsevier Science B.V.

Keywords: Ammoxidation of 3-picoline; Monolayer coverage; Electron spin resonance; Coordinatively unsaturated site

1. Introduction

Vanadia catalysts have been found to be suitable for selective oxidation [1–6] and ammoxidation [7–9] reactions. There are several isolated publications [10–16] on the application of spectroscopic techniques for the characterisation of active phase and adsorbed molecules [17,18] on these catalysts. A detailed study of the various surface species of one series of V_2O_5/TiO_2 catalysts used for ammoxidation of 3-picoline [19] with a wide range of vanadia loadings is the

---

*Corresponding author. Fax: +91 40 717 3387; e-mail: pkr@csiict.ren.nic.in

PII S0926-860X(97)00289-5

objective of the present investigation. The fresh calcined catalysts whose preparation was reported earlier [19], were characterized by the application of SEM, ESR, DTA and chemisorption techniques. Both fresh and used catalysts were studied by FTIR technique with a view to ascertain the nature of different species on the vanadia phase and the modifications that occur during the course of the reaction.

2. Experimental

2.1. Spectroscopic studies

SEM studies of the catalysts were carried out using Hitachi Model S-520 (Japan) Scanning Electron Microscope at an applied voltage of 15 kV. The catalyst samples were mounted on aluminum stubs and were coated with gold in Hitachi HUS-5 GB vacuum evaporator. FTIR spectra of the catalysts were recorded on Nicolet-740 FTIR spectrometer. Self supporting discs were prepared from a mixture of KBr and catalysts by applying pressure for recording FTIR spectra. The FTIR spectra of the catalysts were recorded at room temperature. The pretreatment conditions of the catalysts were the same as for the ammoxidation reactions [19]. ESR spectra of the catalysts were recorded on a Bruker ER 2000-SRC X-band spectrometer with 100 kHz modulation at ambient temperature.

2.2. Thermal analysis studies

Differential thermograms of the samples were obtained on a Leeds&Northrup DTA unit (USA) in the range 25–900°C at a heating rate of 10°C min^{-1}, using α-alumina as a reference material. Grimsha pattern ceramic sample holders and cells were used for this purpose.

2.3. NH_3 and O_2 chemisorption studies

Chemisorption capacities of the catalysts for NH_3 and O_2 were determined using an all glass high vacuum system capable of attaining pressures as low as 10^{-6} torr. The catalysts were reduced in H_2 at 450°C for 2 h prior to O_2 chemisorption which was studied at 'acetone+dry ice' bath temperature (−78°C) following the method of Parekh and Weller [20]. The catalysts were degassed at 150°C for 2 h and then NH_3 chemisorption was carried out at ambient temperature (25°C) by the double isotherm method [21].

3. Results and discussion

3.1. SEM results

The scanning electron micrographs of pure titania (anatase) and pure V_2O_5 are given in Figs. 1 and 2, respectively, and those of fresh calcined catalysts are given in Fig. 3.

SEM studies on supported vanadia catalysts are few in the literature [10,11,22,23]. From Fig. 1 it appears that pure titania (anatase) contains a fine aggregate structure or a highly porous structure. Fig. 2 shows that pure vanadia has needles, flakes and bulk structures. The electronmicrographs of the catalysts with V_2O_5 loading from 2.3 to 3.4 mol% (Fig. 3(C) and (D)) show that the catalysts have a very fine dispersion of vanadia on aggregates of TiO_2. The SEM photographs of 0.4 and 1.3 mol% V_2O_5 catalysts are not shown in the figure. The porous structure of anatase has been obscured by vanadia. However, Backhaus et al. [11] have observed the formation of long needle-like structures or whiskers of V_2O_5 after calcining 0.5% V_2O_5/anatase catalyst at 450°C for 10 h. With increasing V_2O_5 content the whiskers become smaller.

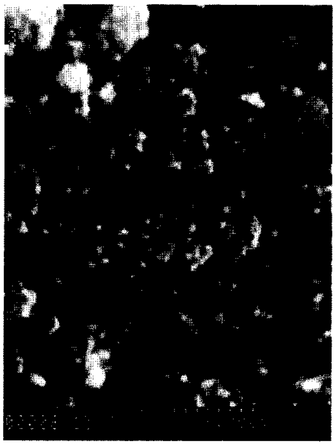

Fig. 1. SEM photograph of pure anatase.

Fig. 2. SEM photograph of pure V_2O_5.

This effect continued with increasing V_2O_5/anatase ratio where bulk structures were observed. A comparision of the results of catalysts with V_2O_5 content below 3.4 mol% in the present case and those of Backhaus et al. [11] suggest that they might have used a low surface area titania/(anatase) support.

The surface area of V_2O_5/TiO_2 (anatase) catalysts has decreased from 79 to 55 $m^2 g^{-1}$ when V_2O_5 loading is increased from 0.4 to 3.4 mol%. At 3.4 mol% V_2O_5, the catalyst has shown the highest activity for ammoxidation of 3-picoline [27]. All these observations point to the fact that vanadia is blocking the micropores and is also highly dispersed on the surface of large pores of TiO_2 (anatase) in the present catalysts.

The electronmicrographs of the catalyst beyond 3.4 mol% V_2O_5 (Fig. 3(E–G)) show that needle-like structures and flake-like bulk structures of V_2O_5 do form in the catalysts. Obviously, the formation of these structures has taken place on the external surface of high vanadia containing catalysts. The surface area of the catalysts further declined from 55 to 19.4 $m^2 g^{-1}$ with increase in V_2O_5 loading. Ki-Won Jun et al. [22] have made similar observations in their study.

3.2. *FTIR results*

The FTIR spectra of fresh and used V_2O_5 and NH_4VO_3 are given in Fig. 4(A) and (B). The FTIR spectra of fresh and used V_2O_5/TiO_2 catalysts are given in Figs. 5 and 6, respectively. The time on stream of ammoxidation experiments varied from 20 h to 30 h.

Fresh vanadia (Fig. 4(A)) has exhibited three distinct bands at frequencies 1618, 1006, and 815 cm^{-1}. Inomata et al. [12] have observed similar absorption bands at 1020 and 825 cm^{-1}. The band at 825 cm^{-1} has been assigned to the coupled vibrations of V=O and V–O–V. The bands at 1020 and 840 cm^{-1} are assigned to the V=O stretching frequency and deformation of V–O–V bridges, respectively, by Frederickson and Housen [24]. Inomata et al. [12] and Nakagawa et al. [13] have assigned the band at 1006 cm^{-1} to stretching vibration of V=O. Tarama et al. [25] and Khulbe et al. [26] have observed V_2O_5 absorption bands at 1019 and 800 cm^{-1}. The used V_2O_5 is observed to give a completely different spectrum (Fig. 4(B)). The bands at 1644, 1015, and 562 cm^{-1} can certainly be attributed to V_2O_4 phase formed due to reduction of V_2O_5 during the course of reaction. Hausinger et al. [27] have shown that presence of water vapour accelerates the formation of polyvanadate groups. Therefore the band at 1404 cm^{-1} may be attributed to the scissoring vibration of NH_4^+ ions present in the compounds like NH_4VO_3 and $NH_4V_4O_{10}$ [28]. The band at 1404 cm^{-1} in reference spectra of pure NH_4VO_3 (Fig. 4C) further confirms our observation. The XRD results of the used catalysts after ammoxidation of 3-picoline have confirmed the presence of these compounds which were reported in our earlier communication [19].

The spectral characteristics of used catalysts are altogether different from those of the fresh catalysts. This observation suggests that drastic changes have taken place in vanadia phase of the catalyst during the reaction.

The band at 1010–1039 cm^{-1}, commonly occurring in the spectra of the fresh catalysts, should be ascribed to the stretching frequency of VO_x units and VO_x clusters [29]. The intensity of the bands at 1600–1630 cm^{-1} and 3300–3700 cm^{-1} (not shown in the figure) which may be ascribed to deformation vibrations of adsorbed water and surface OH groups, respectively, decreases as the amount of adsorbed water and the number of OH groups decrease on anatase surface as it is being progressively covered by increasing vanadia species. The bands at 1340–

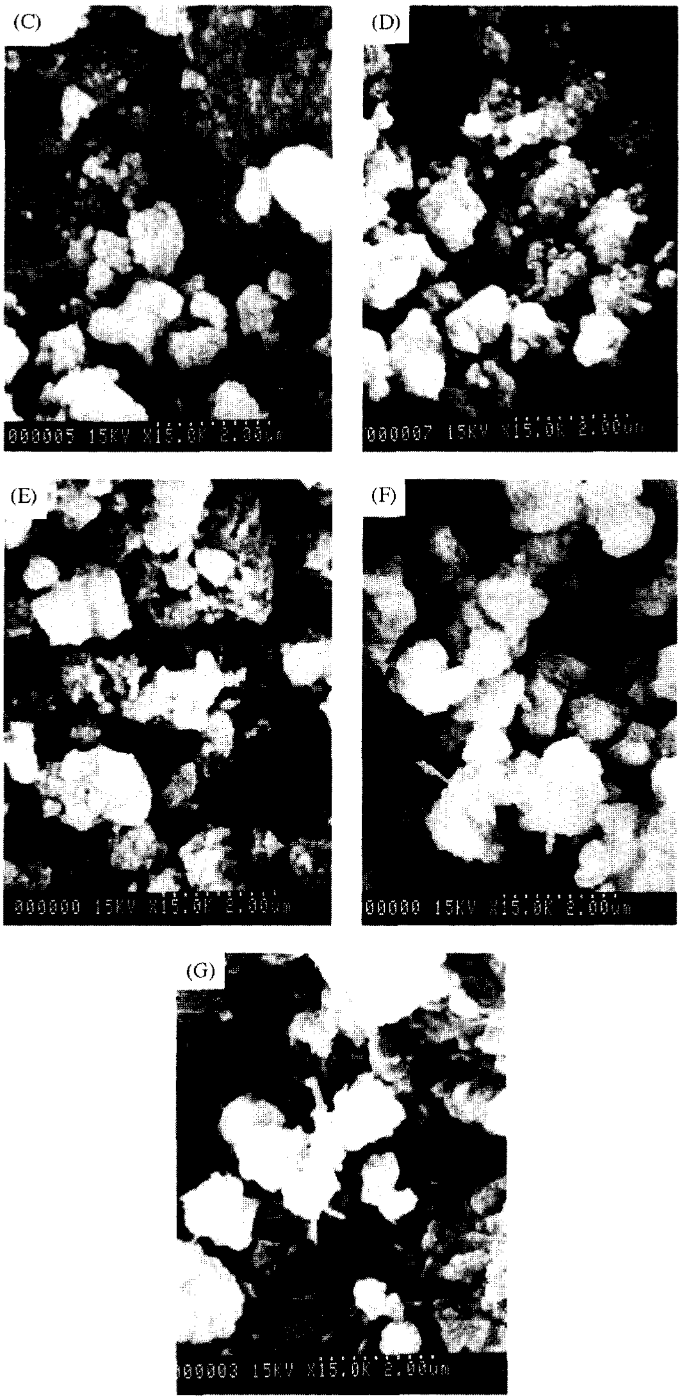

Fig. 3. SEM photographs of fresh V_2O_5/TiO_2 (anatase) catalysts with different V_2O_5 loadings. (C) 2.3 mol%; (D) 3.4 mol%; (E) 4.7 mol%; (F) 5.9 mol%.; (G) 7.2 mol%. Note: The SEM photographs of the catalysts with 0.4 mol% (A); 1.3 mol%; and 9.9 mol% V_2O_5 loadings are not given.

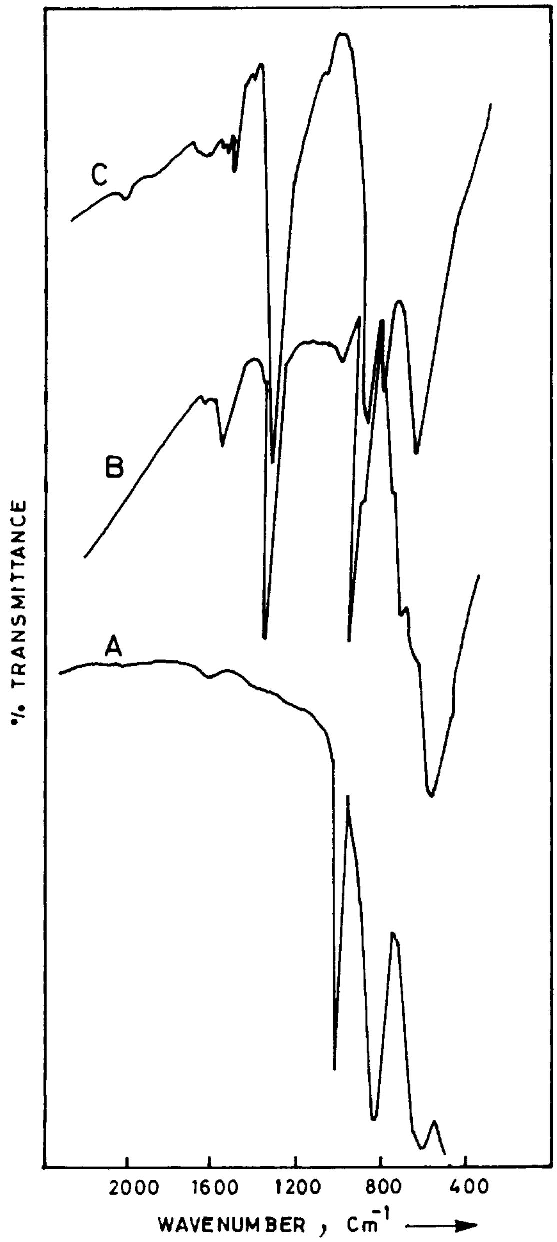

Fig. 4. FTIR spectra of pure V_2O_5. (A) fresh V_2O_5; (B) used V_2O_5; (C) pure NH_4VO_3.

1378 cm^{-1} in the spectra of fresh low vanadia catalysts (Fig. 5(A–D)) can be assigned to anatase phase [29]. The intensity of this band also diminishes at higher vanadia loadings.

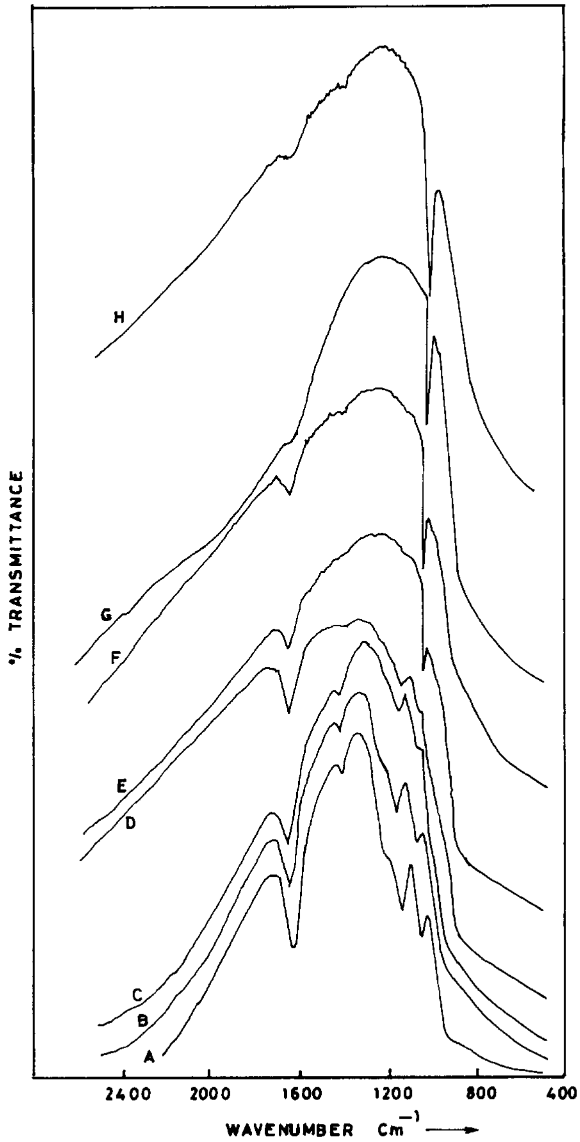

Fig. 5. FTIR spectra of fresh V_2O_5/TiO_2 catalysts with different V_2O_5 loadings. (A) 0.4 mol%; (B) 1.3 mol%; (C) 2.3 mol%; (D) 3.4 mol%; (E) 4.7 mol%; (F) 5.9 mol%; (G) 7.2 mol%; (H) 9.9 mol%.

The intensity of the band at 1630–1658 cm^{-1} decreases while that of the band at 1402–1433 cm^{-1} increases wth V_2O_5 loading in the spectra of used catalysts (Fig. 6). Inomata et al. [12,30] and Takagi et al. [31] have ascribed the latter band to NH_4^+ ions. In the used catalysts NH_4^+ ions are present in adsorbed form and also in the form of compounds like NH_4VO_3 [19,29]. The bands at 1630–1658 cm^{-1}

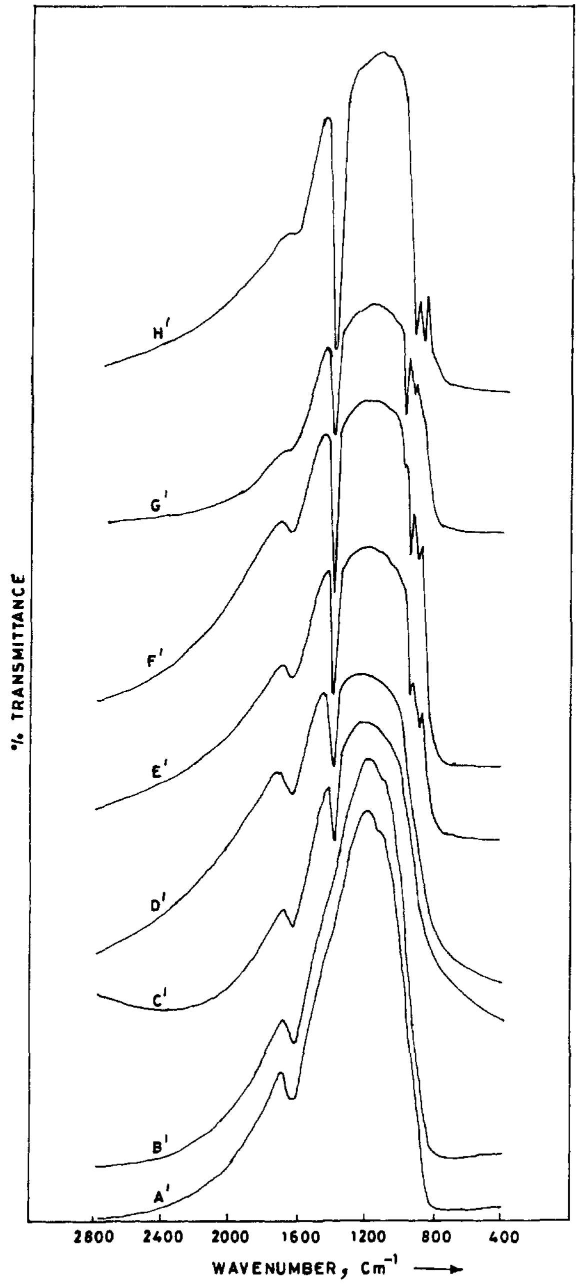

Fig. 6. FTIR spectra of used V_2O_5/TiO_5 catalysts. V_2O_5 concentrations are the same as in Fig. 5. The prime (′) indicates used catalysts.

should be those of coordinatively bonded NH_3 on VO_x clusters [12]. The bands at 994 and 940 cm^{-1} in 7.2 mol% V_2O_5 catalyst (Fig. 6G) can be attributed to surface VO_x species.

The intensity of the bands at 948 and 885 cm^{-1} is observed to increase with vanadia loading in the spectra of used catalysts. These can be attributed to symmetric stretching vibrations of V=O bonds of VO_x clusters [32,33].

3.3. ESR results

Several investigators [34–38] have carried out electron spin resonance (ESR) studies on supported vanadia catalysts. A detailed study of different aspects of electron spin resonance of V_2O_5/TiO_2 system has not been done so far. In the present work, ESR measurements were carried out with a view to investigate the influence of vanadia loading on the co-ordination geometry of vanadium oxide structures and the electron delocalization of anatase supported V_2O_5 catalysts. The ESR spectra of the catalysts with V_2O_5 loading in the range 0.4–9.9 mol% are presented in Fig. 7.

The spectra were analysed using an axial symmetric spin Hamiltonian, H [14,15],

$$H = \beta(g_{\parallel} H_z S_z + g_{\perp} H_x S_x + g_{\perp} H_y S_y) + A_{\parallel} S_z I_z + A_{\perp}(S_x I_x + S_y I_y) \qquad (1)$$

where β is the Bohr Magneton, $g_{\parallel}$ and $g_{\perp}$ are the parallel and perpendicular principal components of the g^{-} tensor, H_x, H_y, H_z are the components of the magnetic field, S_x, S_y, S_z and I_x, I_y, I_z are the components of the spin operators of the electron and the nucleus, respectively. The number of ESR absorption peaks is given by 2I+1 values of m_I, where m_I is the spin quantum number of the nucleus and the magnetic field positions of the peaks that occur are given by

$$H_{\parallel} = 2H_0/g_{\parallel} - (A_{\parallel}/g_{\parallel}\beta)m_I \quad (\text{for } \Theta = 0) \qquad (2)$$

$$H_{\perp} = 2H_0/g_{\perp} - (A_{\perp}/g_{\perp}\beta)m_I \quad (\text{for } \Theta = \Pi/2) \qquad (3)$$

where Θ is the angle between symmetry axis of paramagnetic species and the applied magnetic field (H). By plotting the magnetic field of the observed peaks corresponding to either $H_{\parallel}$ or $H_{\perp}$ against the values of the nuclear spin quantum number M_I, one can obtain a linear relation as shown in Fig. 8. The slopes and the intercepts with the m_I=0 line have been used to derive the values of the desired parameters like $g_{\parallel}$, $A_{\parallel}$, $g_{\perp}$ and $A_{\perp}$ etc. These values and other parameters calculated from them are given in Table 1.

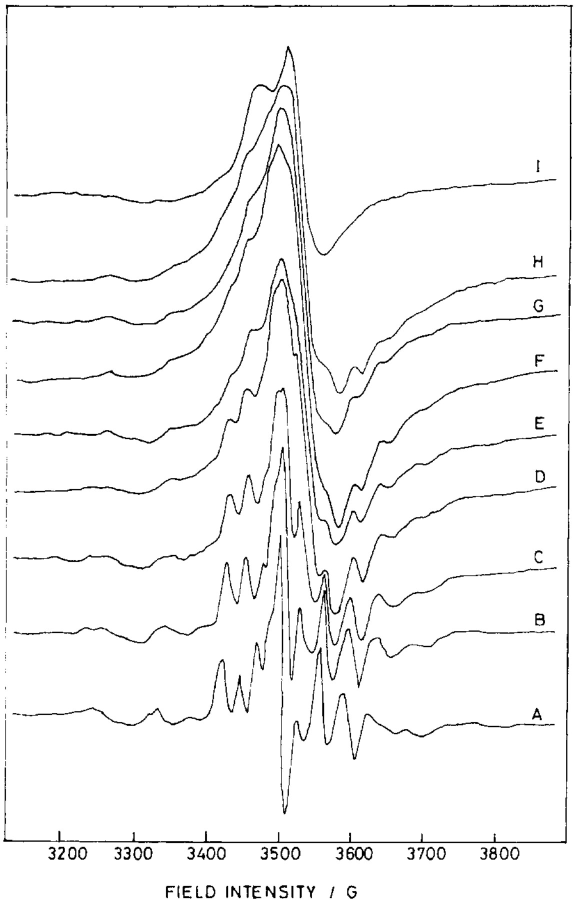

Fig. 7. ESR spectra of fresh V_2O_5/TiO_2 catalysts. V_2O_5 concentrations are the same as in Fig. 5. (I) Pure V_2O_5.

They show that the g tensor of V^{4+} ions exhibits axial symmetry and the parallel components are smaller than the perpendicular ones ($g_{\|}<g_{\perp}$). This fact shows that the catalysts have V^{4+} ions in distorted octahedral or possibly in square pyramidal geometry. It can also be seen from Table 1 that the difference between $g_{\perp}$ and $g_{\|}$ is very small, because Δ (the energy of separation between the energy levels T and E in a crystal field) seems to be large [39,40]. The energy of separation (Δ) is related to g factor by the following expressions:

$$g_{\|} = g_e - 8\lambda/\Delta_1;\; g_{\perp} = g_e - 2\lambda/\Delta_2 \qquad (4)$$

where Δ_1 corresponds to $b_2 \rightarrow e_{\Pi}$ transition and Δ_2 to $b_2 \rightarrow b_1$ transition. The variation in these values occurs because of the variation in the ligand environment of V^{4+} as the concentration of V_2O_5 changes. This in turn causes changes in the values of Δ leading to variation in g values.

From Fig. 7, it is clear that for the catalyst with lowest loading (0.4 mol% V_2O_5), the V^{4+} ions can be considered to exist in diluted conditions. Therefore hyperfine lines are well resolved. As the concentration of V_2O_5 increases the number of V^{4+} ions increases, particularly in the presence of TiO_2. This results in the strong coupling among V^{4+} dipoles leading to exchange interactions among them. This results in the smearing out of hyperfine splittings (hfs) progressively as the concentration of V_2O_5 goes up from 0.4 to 9.9 mol% where the spectrum nearly corresponds to a broad single line without well-resolved hyperfine structures.

Table 1
Spin Hamiltonian parameters measured by EPR for V_2O_5/TiO_2 catalysts

S. No.	Vanadia content (mol%)	$g_{\|}$	$g_{\perp}$	$\Delta G_{\|}/10^{-3}$	$\Delta g_{\perp}/10^{-3}$	B	$\Delta g^a/10^{-3}$	$\Delta g^b/10^{-3}$	$A_{\|}$ (Gauss)	$A_{\perp}$ (Gauss)	$A_{\|}/A_{\perp}$	ΔA	β_2^{*2}
1	0.4	1.985	1.995	17.3	7.3	2.37	10	11.3	155	50	3.10	105	0.65
2	1.3	1.983	1.991	19.3	11.3	1.71	8	14.3	154	50	3.08	104	0.64
3	2.3	1.983	1.995	19.3	7.3	2.64	12	11.3	154	49	3.14	105	0.64
4	3.4	1.966	1.991	36.3	11.3	3.21	25	19.3	157	49	3.20	108	0.65
5	4.7	1.974	1.989	28.3	13.3	2.13	15	13.3	148	49	3.02	99	0.60
6	5.9	1.971	1.986	31.3	16.3	1.92	15	21.3	149	48	3.10	101	0.61
7	7.2	1.977	1.984	36.3	18.3	1.98	18	24.3	149	47	3.17	102	0.62
8	9.9	1.966	1.983	36.3	19.3	1.88	17	25.3	149	47	3.17	102	0.61

$\Delta g_{\|}=g_e-g_{\|}$, $\Delta g_{\perp}=g_e-g_{\perp}$, $B=\Delta g_{\|}/\Delta g_{\perp}$
$\Delta g^a=g_{\perp}-g_{\|}$; $\Delta g^b=g_e-g_0$; $\Delta A=A_{\|}-A_{\perp}$

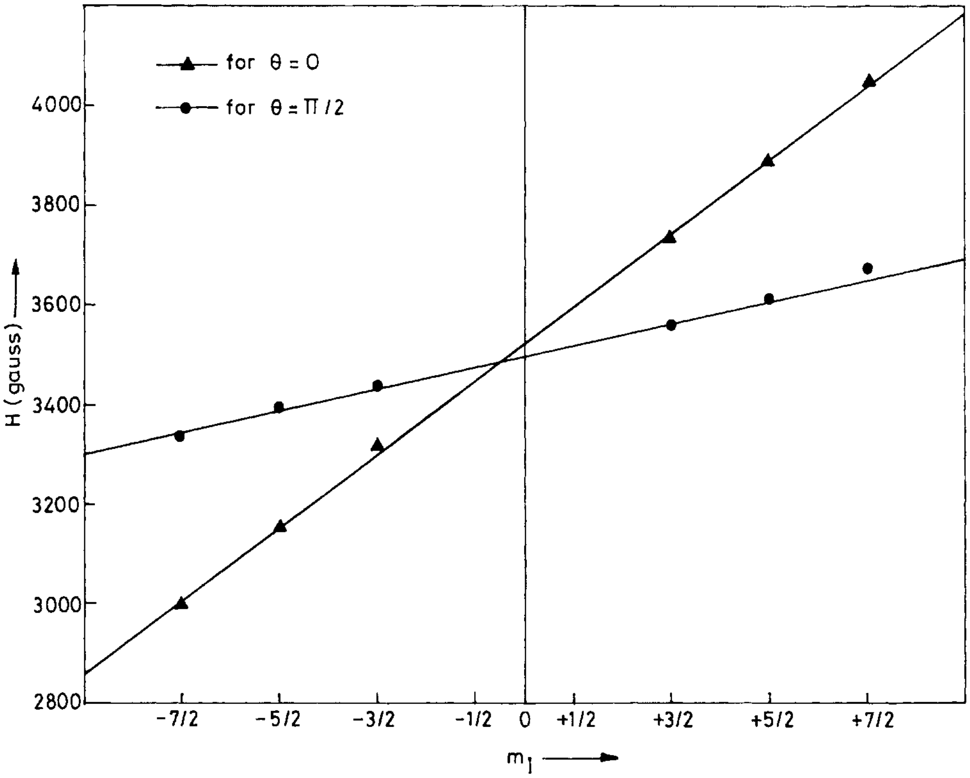

Fig. 8. Magnetic field (H) vs nuclear quantum number, m_I for 0.4 mol% V_2O_5 catalyst.

Fig. 9 shows the factors Δg^a $(g_\perp - g_\parallel)$ and the quantity B $(\Delta g_\parallel / \Delta g_\perp)$, where $\Delta g_\parallel = g_e - g_\parallel$ and $\Delta g_\perp = g_e - g_\perp$ are plotted against vanadia loading of the catalysts. It is interesting to note that both the curves pass through maxima at a V_2O_5 loading of 3.4 mol%, which corresponds to the formation of monolayer of the active phase on the surface of the support. This indicates that the degree of distortion is higher in the case of 3.4 mol% V_2O_5 catalyst, which may be due to high dispersion of VO_x species on the surface of the support. According to Sharma et al. [41], the quantity B reflects changes in the tetragonal distortion. An increase of B indicates a shortening of V=O bond along the principal axis or a lengthening of the distance to the in-plane oxygen ligands in the basal plane. An increasing distance between the four electron-rich-ligands and the central vanadium ion will in return result in a stronger coulomb attraction of vanadyl oxygen. Therefore, the observed variation in B should be related to the changes in both geometries (in-plane and $\perp^r$ to the plane) of VO^{2+}. These in turn give rise to the observed consequences for the activity of the catalyst as they both correspond to the strengthening of V=O bonds. However, Deo and Wachs [4] have not found a correlation between the methanol oxidation activity and the terminal V=O bond strength in monolayer vanadia catalysts supported on various oxides like TiO_2, Al_2O_3 and ZrO_2. They have assumed that the activity of the catalyst depends on the reactivity of the oxygen in the V–O-support bond. The results of the present ESR study seem to lend support to their contention. It appears that the shortening and strengthening of the terminal V=O bond results in the lengthening and weakening of the V–O-support bond at a monolayer coverage because of which the oxygen in this bond becomes more reactive and the catalyst exhibits the highest ammoxidation activity.

It is worth commenting on the ratio of the hyperfine coupling constants $(A_\parallel / A_\perp)$, which reached a maximum value of 3.2 (Table 1) at 3.4 mol% V_2O_5 loading, which is a monolayer catalyst. This is certainly consistent with changes observed for g-parameter and

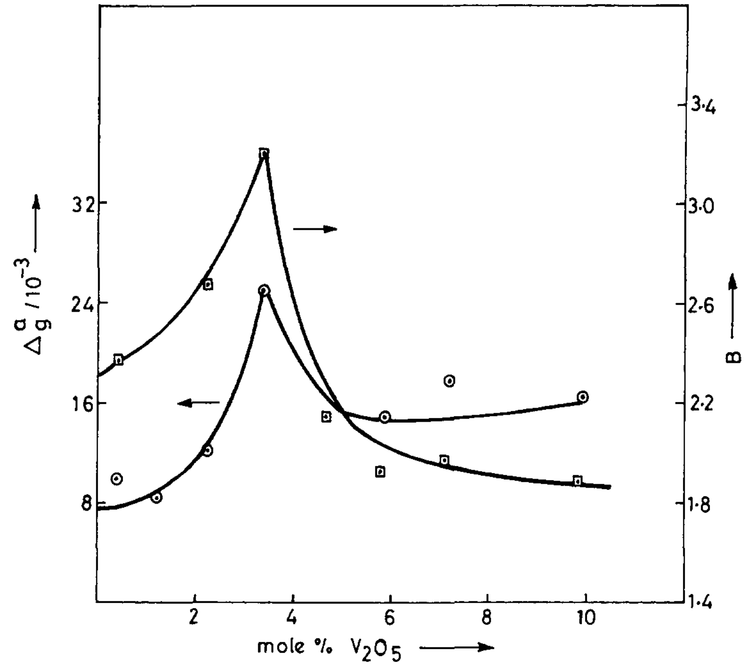

Fig. 9. Variation of ΔG^a ($g_\perp - g_\parallel$) and the quantity B ($\Delta g_\parallel / \Delta g_\perp$) as a function V_2O_5 loading.

correlates well with the vanadia loading giving the highest ammoxidation activity at 3.4 mol% [19].

Another parameter which also reflects the observed significance for 3.4 mol% V_2O_5 catalyst is β^{*2} [36] which is given by

$$\beta^{*2} = 7/6\Delta g_\parallel - 5/12\Delta g_\perp - 7/6(A_\parallel - A_\perp/P)$$

A value of P=184.5 G [42] has been used in the calculations.

It is interesting to observe that β^{*2} remains almost constant at 0.65 (Table 1) up to a V_2O_5 loading of 3.4 mol% and then decreases to 0.61 which again remains constant in the catalysts with V_2O_5 loadings at and above 4.7 mol%. This could also be attributed to the formation of highly dispersed VO_x species on the catalysts with low vanadia contents.

3.4. *Differential thermal analysis results*

The differential thermograms of the catalysts are presented in Fig. 10. The thermograms contain only endothermic peaks. The intensity of the endothermic peak from 100–150°C is the highest for 0.4 mol% V_2O_5 catalyst (A) and decreases as the vanadia content increases. Catalyst (A) has maximum amount of adsorbed water on its surface and this decreases as anatase surface is gradually interacted and covered by increasing amounts of vanadia. A second endothermic peak appears at 630–675°C in the thermogram of 3.4 mol% V_2O_5 catalyst (D) and its intensity increases with vanadia loading. Bond et al. [16] have ascribed this peak to melting of vanadia on the catalyst surface. Another endothermic peak appears at 680–750°C in the thermograms of the catalysts with V_2O_5 loadings at and above 5.9 mol%. Bond et al. [16] have also observed this peak and ascribed it to the process of oxygen loss.

3.5. *NH_3 and O_2 chemisorption*

The O_2 and NH_3 uptakes per unit surface area of the catalysts along with their BET surface areas are presented in Table 2. The irreversible O_2 uptakes at −78°C on the reduced catalysts and the NH_3 uptakes at ambient temperature on the catalysts degassed at 150°C are presented in Fig. 11. It is clearly seen from the figure that the chemisorption of both the adsorbate gases increases with V_2O_5 loading and passes through

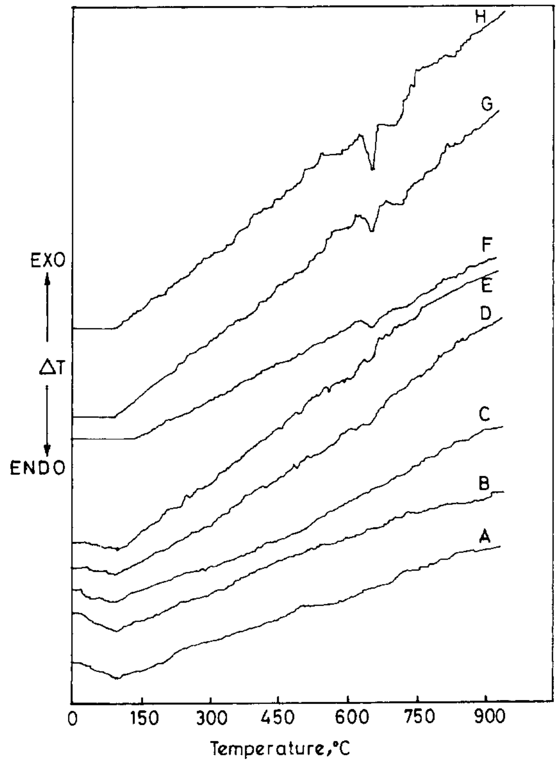

Fig. 10. Differential thermograms of V_2O_5/TiO_2 catalysts. V_2O_5 concentrations are the same as in Fig. 5.

a maximum at 3.4 mol% V_2O_5 loading and thereafter declines considerably. The change in the trend of chemisorption of the gases is the same as the ammoxidation activity of these catalysts up to 3.4 mol% V_2O_5 reported in the earlier communication [19]. Rao and Narsimha [43] have observed a similar correlation between the irreversible uptakes of these gases and methanol oxidation activity of V_2O_5/TiO_2 catalysts. According to Kantcheva et al. [44] isolated monooxovanadyl groups and two-dimensional vanadium oxide clusters exist at low vanadia coverages at and below a monolayer. A separate V_2O_5 phase and polyvanadates are observed at higher coverages on V_2O_5/TiO_2 catalysts. The very high NH_3 uptakes indicate that NH_3 chemisorption occurs on Lewis acid sites (V=O) as well as on Bronsted acid sites (V–OH). NH_3 is coordinated to V^{5+} ions causing rearrangement in the VO_x surface species [44]. The adsorption sites for NH_3 increase with increase in monomeric VO_x units and the two-dimensional structures as the V_2O_5 concentration increases up to a monolayer coverage. The coordinatively unsaturated sites (CUS) on V^{4+} ions which chemisorb oxygen irreversibly also go on increasing up to a monolayer coverage.

The adsorption sites of NH_3 and O_2 per g of catalyst gradually decrease as crystalline V-oxides and polyvanadates are formed when V_2O_5 concentration is

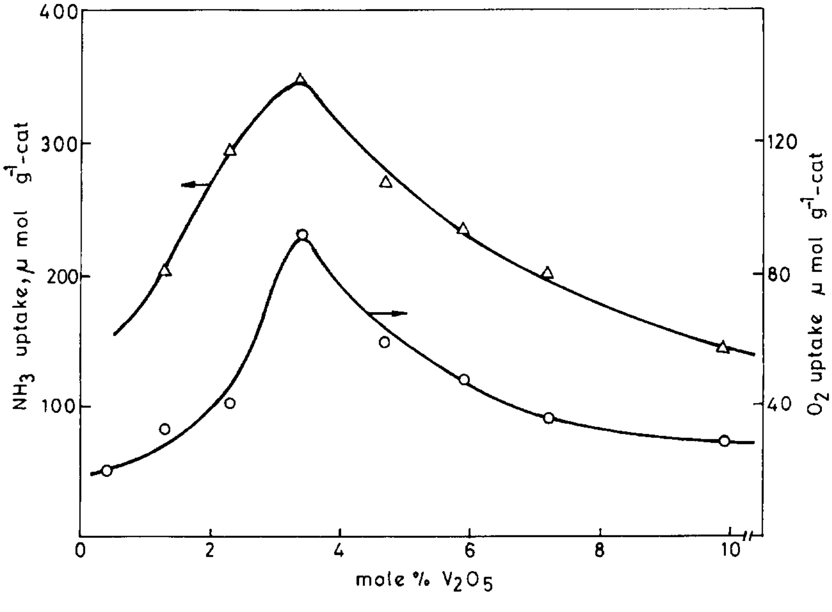

Fig. 11. Irreversible O_2 and NH_3 uptakes vs V_2O_5 loadings of V_2O_5/TiO_2 catalysts.

Table 2
Results of surface area, oxygen and ammonia uptakes over V_2O_5/TiO_2 (anatase) catalysts

Catalyst mol% V_2O_5	BET surface area $m^2\,g^{-1}$	O_2 uptake μ mol m^{-2}	NH_3 uptake μ mol m^{-2}
0.4	76.0	0.30	2.4
1.3	69.8	0.47	2.0
2.3	58.5	0.69	5.1
3.4	55.1	1.60	5.9
4.7	39.8	1.70	6.4
5.9	28.3	1.70	8.4
7.2	18.6	1.70	9.2
9.9	19.3	1.70	9.4

increased beyond 3.4 mol% (Fig. 11). However, the adsorption site densities per unit surface area of the catalysts remained more or less constant beyond 3.4 mol% vanadia loading (Table 2). According to Bond et al. [45], the joint effect of the V=O and V–OH groups determines the good catalytic properties of V_2O_5/TiO_2 (anatase) catalysts in selective oxidation reactions [46]. Perhaps such an effect is very much pronounced in a monolayer catalyst for ammoxidation reaction also. From the isotopic transient studies Janssen et al. [17] have concluded that the monolayer catalyst has the highest exchangeability of oxygen. The highest participation of lattice oxygen in a monolayer catalyst is perhaps responsible for its highest chemisorption capacity and for ammoxidation activity [19].

4. Conclusions

The spectroscopic studies of V_2O_5/TiO_2 catalysts reveal that gradual changes take place in the structure of vanadia phase with the increase in vanadia concentration. SEM studies indicate that deposition of vanadia occurs inside the mesopores of TiO_2 (anatase) till the monolayer coverage (3.4 mol% V_2O_5). FTIR spectra of fresh catalysts are characteristic of highly dispersed VO_x species and two-dimensional structures at and below monolayer coverage of vanadia. The spectra of used catalysts show that drastic changes have taken place in the structure of the active phase during the course of the reaction. The hyperfine structure of the ESR spectra of fresh catalysts reveal that vanadium is in a highly dispersed form in the catalysts up to a monolayer coverage where the catalyst has exhibited the highest ammoxidation activity. The DTA studies have shown three endothermic peaks corresponding to desorption of adsorbed water, melting of vanadia and evaporation of oxygen from vanadia. Chemisorption of ammonia and oxygen is observed to be maximum on a monolayer catalyst just as the ammoxidation activity of the catalyst indicating the existence of a maximum number of adsorption sites.

Acknowledgements

Two of the authors, K.V. Narayana and A. Venugopal, record their grateful thanks to CSIR, India, for the award of Senior Research Fellowships. Thanks are also due to Prof. M. Salagram, Department of Physics, Osmania University, Hyderabad, India, for his help in the interpretation of ESR results.

References

[1] D.J. Hucknail, Selective Oxidation of Hydrocarbons, Academic Press, London, 1974.
[2] D.B. Dadyburger, S.S. Jewar, E. Ruckenstein, Catal. Rev. Sci. Eng. 19 (1979) 293.
[3] J.R. Sohn, Y.I. Pae, M.Y. Park, S.G. Jo, React. Kinet. Catal. Lett. 55 (1995) 325.
[4] G. Deo, I.E. Wachs, Crit. Rev. Surf. Chem. 4 (1994) 141.
[5] I.E. Wachs, R.Y. Saleh, S.S. Chan, C.C. Chersich, Appl. Catal. 15 (1985) 339.
[6] C.R. Dias, M.F. Portela, G.C. Bond, J. Catal. 157 (1995) 344.
[7] Y. Murakami, M. Niwa, T. Hattori, S. Osawa, I. Igushi, H. Ando, J. Catal. 49 (1977) 83.
[8] A. Andersson, J. Catal. 76 (1982) 144.
[9] A. Andersson, S.T. Lundin, J. Catal. 65 (1980) 9.
[10] E.L. Kugler, D.P. Leta, J. Catal. 109 (1988) 387.

[11] K.G. Backhaus, R. Haass, U. Illgen, J. Richter-Mendau, J. Scheve, I.J. Schuls, K. Thiessen, J. Velter, Inter. Sym. On Reactivity of Solids, (1984), Dijon 1, France.

[12] M. Inomata, A. Miyamoto, Y. Murakami, J. Catal. 62 (1990) 140.

[13] Y. Nakagawa, J. Ono, H. Miyata, Y. Kubokawa, J. Chem. Soc. Faraday Trans. 1 79 (1983) 2929.

[14] H. Takahashi, M. Shiotani, H. Kobayashi, J. Sohma, J. Catal. 14 (1969) 134.

[15] B. Bleaney, Phil. Mag. 42 (1951) 441.

[16] G.C. Bond, A.J. Sarkani, G.O. Parfitt, J. Catal. 57 (1979) 476.

[17] F.J.J.G. Janssen, F.M.G. van Den Kerkhof, H. Bosch, J.R.H. Ross, J. Phys. Chem. 91 (1987) 5921.

[18] M. Inomata, K. Mori, A. Miyamoto, T. Ui, Y. Murakami, J. Phys. Chem. 87 (1983) 754.

[19] K.V. Narayana, A. Venugopal, K.S. Rama Rao, V. Venkat Rao, S. Khaja Masthan, P. Kanta Rao, Appl. Catal., A 150 (1997) 269.

[20] B.S. Parekh, S.W. Weller, J. Catal. 47 (1977) 100.

[21] S. Khaja Masthan, K.V. Narayana, V. Venkat Rao, P. Kanta Rao, Ind. J. Chem. Technol. 3 (1996) 313.

[22] B. Jonson, B. Rebenstorf, R. Larsson, J. Chem. Soc. Faraday Trans. 1 84 (1988) 1897.

[23] Ki-Won Jun, Kyu-Wan Lee, H. Chan, Appl. Catal. 63 (1990) 267.

[24] L.D. Frederickson, D.M. Housen, Anal. Chem. 35 (1963) 818.

[25] K. Tarama, S. Teranishi, S. Yoshida, N. Tamara, Proc. Inter. Cong. 3rd, Amsterdam, 1965, p. 202.

[26] K.C. Khulbe, R.S. Munn, A. Manoojian, J. Chem. Phys. 60 (1974) 48.

[27] G. Hausinger, H. Schemlz, H. Knozinger, Appl. Catal. 39 (1988) 267.

[28] S. Kittaka, H. Hamaguchi, T. Umezu, T. Endoh, T. Takenaka, Langmuir 13 (1997) 1352.

[29] R.A. Nyquist, R.O. Kasel, Infrared Spectra of Inorganic Compounds, Academic Press, New York and London, 1971, p. 305.

[30] M. Inomata, A. Miyamoto, Y. Murakami, Chem. Lett. (1978) 441.

[31] M. Takagi, T. Kawai, M. Soma, T. Onishi, K. Tamaru, J. Catal. 50 (1977) 441.

[32] I.E. Wachs, J. Catal. 124 (1990) 570.

[33] C. Cristiani, P. Forzatti, G. Busca, J. Catal. 116 (1989) 586.

[34] B.G. Silobernagel, J. Catal. 56 (1979) 315.

[35] H. Eckert, I.E. Wachs, Mat. Res. Soc Sym. Proc. Vol. 3 (1988) 459.

[36] G. Busca, P. Tittarelli, E. Tronconi, P. Forzatti, J. Solid State Chem. 67 (1987) 91.

[37] Y. Kera, T. Inoue, Y.M. Kaze, Bull. Chem. Soc. Jpn. 61 (1988) 761.

[38] M. Rusieka, B. Grazybcwska, M. Gasior, Appl. Catal. 10 (1984) 101.

[39] M. Salagram, N. Satyanarayana, S. Radha Krishnan, Polyhedron 5 (1986) 1171.

[40] J.E. Wertz, J.R. Bolton, Electron Spin Resonance: Elementary Theory and Practical Applications; Chapman and Hall, New York. London, 1986, p. 288.

[41] V.K. Sharma, A. Wokaun, A. Baiker, J. Phys. Chem. 90 (1986) 2715.

[42] J.A. McMillan, T. Halpern, J. Chem. Phys. 55 (1971) 33.

[43] P. Kanta Rao, K. Narsimha, in Catalytic Selective Oxidation, ACS Symp. Series 523, S.T. Oyama, J.W. Hightower (Ed.), ACS Washington DC, 1993, p. 231.

[44] M. Kantcheva, K. Hadjiivanov, D. Klissurski, J. Catal. 134 (1992) 299.

[45] G.C. Bond, J.P. Zurita, S. Flamerz, P.J. Gellings, H. Bosch, J.G. van Ommen, B.J. Kip, Appl. Catal. 22 (1986) 361.

[46] K.I. Hadjiivanov, D.G. Klissurski, Chem. Soc. Rev. (1996) 61.